Translational Oncology 14 (2021) 100980

Contents lists available at ScienceDirect

Translational Oncology

journal homepage: www.elsevier.com/locate/tranon

Original Research

Thymic function affects breast cancer development and metastasis by regulating expression of thymus secretions PTMα and Tβ15b1

Dongling Shi[a,1], Yanmei Shui[a,1], Xie Xu[b], Kai He[c], Fengqing Yang[d,*], Jianli Gao[a,*]

[a] Academy of Traditional Chinese Medicine, Zhejiang Chinese Medical University, Hangzhou, Zhejiang 310053, China
[b] College of Pharmaceutical Sciences, Zhejiang Chinese Medical University, Hangzhou, Zhejiang 310053, China
[c] The First Affiliated Hospital, Zhejiang University, Hangzhou, Zhejiang 310009, China
[d] School of Chemistry and Chemical Engineering, Chongqing University, Chongqing 401331, China

ARTICLE INFO

Keywords:
Breast cancer
Thymosin
Tumor metastasis
PTMα and Tβ15b1

ABSTRACT

Breast cancer is currently one of the most common malignant tumors in women. Our previous research found that thymic dysfunction has a certain relationship with the occurrence and development of breast cancer. In order to explore whether the functional status of thymus is related to the development and metastasis of breast cancer, we use BALB/c wild type mice (BALB wt), BALB/c nude mice (BALB nu), BALB wt mice implanted with 4T1 cells (wt 4T1), BALB nu with 4T1 (nu 4T1), D-galactose treatment wt 4T1 mice (D-Gal), Thymalfasin treatment wt 4T1 mice (Tα1), Cyclophosphamide treatment wt 4T1 mice (CTX), Doxorubicin treatment wt 4T1 mice (Dox) in the research. As a result, nu 4T1, D-Gal and DOX had earlier lung metastases. Gene chip results showed that PTMα and Tβ15b1 were the most up-regulated and down-regulated genes in thymosin-related genes, respectively. Overexpression or silencing of PTMα and Tβ15b1 genes did not affect the proliferation of 4T1 cells. PTMα gene silenced, cell migration and invasion ability enhanced, while PTMα gene overexpression, the cell invasion ability weaken. In vivo, PTMα gene overexpression promotes tumor growth and lung metastasis in the early stage, but has no significant effect in the later stage. Tβ15b1 overexpression also promotes tumor growth in the early stage, but suppresses in the later stage. Tβ15b1 gene silencing inhibits tumor lung metastasis. Thus, our findings demonstrated that thymic function affects breast cancer development and metastasis by regulating expression of thymus secretions PTMα and Tβ15b1. Our study provided new directions for breast cancer therapy.

Introduction

Breast cancer is one of the most common malignancies among women worldwide, the most common cause of cancer death in women in underdeveloped areas, and the second among women in more developed regions. How to prevent breast cancer metastasis has become one of the major problems faced by modern medicine [1]. Metastasis of breast cancer is a complex process involving multiple systems of the whole body. It mainly includes two aspects: circulatory system and immune system.

Thymus, as the central immune organ of human body, is the site of oriented differentiation of myeloid/lymphoid cells. It was previously thought that the thymus was gradually degenerated after puberty and replaced by adipose tissue, but studies have found that the thymus of adults still has the function of T cell reconstruction [2]. Studies have found that compared with elderly patients, young breast cancer patients with stronger thymus function and immune function tend to have a higher degree of malignancy, a lower degree of differentiation, a faster course of disease development and a shorter survival period [3,4]. Thymus is mainly composed of thymus cells and thymus stromal cells. The former is the T cells that developed to different stages after pre-T cells from bone marrow enter the thymus, while the latter includes epithelial cells, dendritic cells and macrophages. Lymphocytes, dendritic cells and macrophages are known to be important in tumor immune remodeling and escape, but the relationship between thymus, thymosin and tumor metastasis has not been systematically reported.

Thymosin is an important peptide hormone secreted by thymic stromal cells mainly composed of thymic epithelial cells. It is mainly composed of two major families, α and β. The current research focuses on Thymosin α1 (Tα1), Thymosin β4 (Tβ4), Thymosin β10 (Tβ10) and Thymosin β15 (Tβ15). In addition, the thymus produces a variety of peptide thymic hormones, including thymopoietin, thymulin, lymphocyte slimulating factor and thymic humoral factor. Thymosin acts on thymocytes, differentiation and maturation into T cells of different subpopulations,

* Corresponding authors.
E-mail addresses: fengqingyang@cqu.edu.cn (F. Yang), jianligao@zcmu.edu.cn (J. Gao).
[1] Dongling Shi and Yanmei Shui contributed equally to this work.

https://doi.org/10.1016/j.tranon.2020.100980
Received 23 October 2020; Received in revised form 22 November 2020; Accepted 30 November 2020

and obtains immunological activity. Review of related literature in recent years, we can find that thymosin may play a two-way regulation role in the development of tumors, Tα1 can improve the immune function of chemotherapy patients [5], and can induce the blockade of Akt signaling pathway in tumor cells and activate the p53 pathway, promotes the expression of CDKI while decreasing the expression levels of cyclins and CDKs, and thus arrests the cell cycle in the G1 phase [6], while Tα1 can promote angiogenesis [7]. Tβ4 can enhance the invasion and metastasis of tumor cells and promote angiogenesis [7–9]. Tβ10 inhibits cell invasion and metastasis and may be a potential progression marker for multiple tumors [10,11]. Tβ15 could be used as a marker for early diagnosis of prostate cancer, and its expression was also related to human breast cancer invasion ability [12]. In summary, it can be found that the role of thymosin in the positive or negative regulation of tumorigenesis is still inconclusive. The previous study of the research team found that there is a certain relationship between thymic dysfunction and the development and metastasis of breast cancer. Therefore, we speculate that the thymus may play a very important role in the development of the tumor, perhaps by affecting the secretion of thymosin. This study aims to explore the role of thymic function in the growth and metastasis of breast cancer tumors through in vitro and in vivo experiments.

Materials and methods

Cell and cell culture

Mouse breast cancer cell line 4T1 is an ERα, ERβ positive cell line, which can grow in homologous BALB/c mice and has a high proportion of multiple organ metastasis such as lung, liver and bone. 4T1 cell line (ATCC No. CRL-2539) were purchased from the Institute of Cell Resource Center of the Chinese Academy of Sciences (Shanghai, China).

Mouse breast cancer cell line 4T1-Luc: a stable cell line carrying the firefly luciferase gene, which was infected with a retroviral vector expressing firefly luciferase and antibiotic screening. Briefly, a recombinant retrovirus was packaged in HEK-293 cells by co-transfecting cells with pSEB-Luc and pAmpho packaging plasmid using Lipofect AMINE (Invitrogen, life technologies, CA, USA). The firefly luciferase activity was confirmed by using Promega's Luciferase Assay kit (Promega, Madison, WI, USA).

4T1 and 4T1-Luc were cultured in Dulbecco's modified Eagle's medium (DMEM) (Gibco, Life Technologies, USA) supplemented with 10% fetal bovine serum (Gemini, Woodland, CA, USA) and 100 Units penicillin/streptomycin (Genom Bio-pharmaceutical Tech. Co., Ltd., Hangzhou, Zhejiang, China) at 37°C in a 5% CO_2, 0.25% trypsin and 0.02% EDTA were purchased from Genom Bio-pharmaceutical Tech. Co., Ltd.

In vitro gene transfection and stable cell line screening of 4T1-Luc cells. Unloaded control adenovirus group expressing green fluorescent protein (Ad-GFP), Ad-PTMα and Ad-Tβ15b1 were cloned into the p-AD-Amp vector and packaged with adenovirus (Vigene Biosciences.INC, Shandong, China). No-load control lentivirus group expressing green fluorescent protein (Si-GFP), PTMα-shRNA, and Tβ15b1-shRNA were used to clone the target gene into pLent-U6-GFP-Puro vector, lentiviral packaging (Vigene Biosciences.INC, Shandong, China). And screening with an appropriate concentration of puromycin (Sigma-Aldrich, USA).

Animals

Experimental BALB/c mice and BALB/c nude mice (6-8 weeks old, female, 18-20 g) were purchased from Vital River Laboratory Animal Technology Co. Ltd. (Beijing, China) and maintained at the animal facility of Experimental Animal Research Center of Zhejiang Chinese Medical University. All procedures were performed according to protocols following the guidelines for the Use and Care of Laboratory Animals published by the Zhejiang Province (2009) and approved by the Animal Ethics Committee of Zhejiang Chinese Medical University. All mice were maintained in SPF environment with access to food and water *ad libitum*.

Breast cancer bearing mice model

After a week of adaptive feeding, BABL/c mice were grouped randomly (n=10/group). After mice were anesthetized with 2% isoflurane, breast cancer bearing mice model was conducted as described previously [13]. In brief, 4T1-Luc cells were harvested resuspended in phosphate-buffered saline (PBS) ($\sim 1 \times 10^6$ 4T1-Luc cells in 100μl PBS) and inoculated in BALB/c and BALB/c nude mice on the mammary fat pad (MFP). After 48 hours, start the administration. During the experiment, tumor volume and mice weight were noted every five days. The dimensions of the primary tumor sites were measured using vernier calipers. Tumor volume was calculated using the following equation: Volume = [length (L) + width (W)] x L x W x 0.2618. At the endpoint, mice were sacrifced by carbon dioxide asphyxiation, the thymus, lung, spleen and tumor tissues were dissected, and the organ coefficients were calculated by the equation: Organ index (g/g) = organ weight (g)/body weight (g)*100%. After the lung was fixed with formalin for 48h, the tumor size on the surface of lung tissue was measured with vernier caliper and counted.

Xenogen bioluminescence imaging

After the third week inoculation, Whole-body optical imaging of the mice was performed as previously described weekly [13]. Briefly, mice were intraperitoneally injected with the luciferase substrate 0.1ml. After 5min free activity, anesthetized with isoflurane (2%, 1.5l/min) via a nose-cone mask within a Xenogen IVIS 200 imaging system (Caliper Life Sciences, Hopkinton, MA, USA). Xenogen's Living Image V2.50.1 software (Caliper Life Sciences) was used for quantitative analysis.

Gene chip detection

After 35 days, the tumor tissues of the wt 4T1, D-Gal mice and nu 4T1 (n=3/group) were collected analyzed by gene chip. The specific content was completed by Aksomics Inc..

H&E staining

After the last administration, mice were sacrificed and the thymus, tumor, lung tissues were dissected and fixed in 10% formalin overnight and embedded in paraffin. Hematoxylin-eosin (H&E) staining was carried out in accordance to the respective specification. Slides were photographed with microscope ((Ti-S, Nikon, Japan).

RNA isolation and qPCR analysis of TRECs or thymosin-related gene

To analyze the mRNA levels of thymosin-related genes named Prothymosin α (PTMα), Thymosin beta 15b1(Tβ15b1) in 4T1-Luc cells and thymic function gene T cell receptor rearrangement excision circles (TRECs) in mice peripheral blood cells, Ad-PTMα, Ad-Tβ15b1, sh-PTMα and sh-Tβ15b1 were added to infect 4T1-Luc cells for 24h. Total RNA was isolated with Trizol reagent (Invitrogen) according to the manufacturer's protocol. The tumor masses were excised and immediately stored in liquid nitrogen until required. The frozen tissue was put in an RNase-free mortar and immediately pestle which contained Trizol and total RNA was isolated, and reverse-transcribed according to the manufacturer's protocol. The sequences of the real-time PCR primers are synthesized by Sangon Biotech (Shanghai) Co., Ltd.. Real-time PCR was carried out in a 20μl reaction mixture containing 10μl Hot Start Fluorescent PCR Mix, 8μl ddH_2O, 0.5μl Sense primer, 0.5μl Anti-sense primer and 1μl of cDNA template. The PCR was performed in an Applied Biosystems Step

One Plus™ Real-Time PCR system (Thermo Fisher Scientific, USA) using the following cycle parameters: one cycle of 95°C for 1min, 40 cycles of 95°C for 20s, different Tm temperature for 20s and 72°C for 18s. Data analysis was performed with a comparative Ct method with GAPDH as the endogenous control. Fold-expression changes were calculated using the equation $2^{-\triangle\triangle ct}$. The following primers were used in this study: GAPDH, forward 5'- GGCTGCCCAGAACATCAT -3' and reverse 5'- CGGACACATTGGGGGTAG-3'; TRECs, forward 5'- CATTGCCTTTGAACCAAGCTG -3' and reverse 5'- TTATGCACAGGGTGCAGGTG -3'; PTMα, forward 5'- CATTGTTCCTGGGTCGTGCT -3' and reverse 5'- GCCGCGAGTGAGGGAATTAAA -3'; Tβ15b1, forward 5'- TTGGAACCGGCAGACAAGATG -3' and reverse 5'- ATCTACCAGGAGCTGCCTAACA -3'.

ELISA

Blood was collected from fundus venous plexus at the third and fifth weeks of administration. After standing at room temperature for 2h, the blood was centrifuged and the supernatant was taken. ELISA detected the expression of thymus hormone in peripheral blood according to kit instructions (Yuanye Bio-Technology Co., Ltd, Shanghai).

MTT detection of the ability of cell proliferation

The experiment was divided into blank group, Ad-GFP group, Ad-PTMα group, Ad-Tβ15b1 group, Si-GFP group, PTMα-shRNA group, Tβ15b1-shRNA group. Cell suspension was added into the 96-well plate (about 5×10^3 cells/well), each group consisted of 3 repeated wells. In addition to the blank group, Ad-GFP group and Si-GFP group, the remaining groups were added with 100μL of culture medium containing different adenoviruses / lentiviruses, and cultured for 24h, 48h and 72h respectively. Cell viability was evaluated by the 3-(4, 5-dimethylthiazol-2-yl)-2, 5-diphenyltetrazolium bromide (MTT) assay. The absorbance in each well was measured at 570 nm using a microplate reader (Synergy H1, BioTek, America).

Transwell chamber detection of the ability of cell invasiveness

The Matrigel glue was melted at 4°C a day before the experiment, and Matrigel glue (200-300μg/ml) was diluted with serum-free cold cell culture medium DMEM, and 100μl per well was added. After paving the glue, the room was placed in the 37°C incubator 6h. Then cells were suspended and added in the upper chamber (5×10^4/well), the lower chamber was layered with 500μl 5% FBS DMEM culture medium, 37°C, humidity saturation and 5% CO_2 culture incubator 8h. After 8h culture, the cells were wiped with cotton swabs to the upper layer of the chamber without the glue. The lower layer of the small chamber plus 500μl 0.1% crystal violet solution (Contains 4% polyformaldehyde) was fixed to 30min, and the PBS was cleaned. The stained 4T1-Luc in each well were then counted five different fields with microscope (Ti-S, Nikon, Japan) at a magnification of 100× by two independent investigators.

Wound healing assay

Cell suspension was added into the 24-well plate (about 1×10^5 cells/well), and about 80% of the cells were fused and transfected with Ad-GFP, Ad-PTMα, Ad-Tβ15b1, Si-GFP, PTMα-shRNA, Tβ15b1-shRNA, respectively. After 24h, make a scratch with 10μl tips, PBS cleaning 2 times, gently wash off the cells, replaced by serum-free medium, taking pictures under the microscope (Ti-S, Nikon, Japan) at 0h, 48h and calculate the migration rate (0h width - 48h width / 0h width)×100%.

Statistical analysis

The *in vivo* data were analyzed by one-way ANOVA and the *in vitro* data were analyzed by the non-paired Student's t-test between control group and each treatment group. The Graph-Pad Prism 5 was used. Results are reported as Means ± SD or Means ± SEM. A p-value < 0.05 was considered statistically significant.

Results

Thymus function status has an extremely important relationship with the development and metastasis of breast cancer

Weight, primary tumor volume, lung metastatic sites

To investigate the effect of thymic function changes on the growth and metastasis of breast cancer, 60 female BALB/c mice and 20 female BALB/c nude mice were purchased. And BABL/c mice were randomly divided into 6 groups: BALB wt, wt 4T1, D-Gal, Tα1, CTX, DOX. BALB/c nude mice were randomly divided into 2 groups: BALB nu, nu 4T1. A total of 8 groups (n=10/group). 48 hours after inoculation, D-Gal (100 mg/kg/d, s.c), Tα1 (8 mg/kg/w, s.c), CTX(100 mg/kg/w, i.p), DOX(6.7 mg/kg/w, i.p) were administrated respectively for 35 days. The present study first evaluated the weight, primary tumor volume, lung metastatic sites of the 4T1-Luc mouse breast cancer tumor-bearing mice. Tumor growth was monitored through measuring the tumor volume, and bioluminescence was detected using whole body Xenogen imaging.

With the extension of administration time, the body weight of mice in DOX administration group was lower than that of wt 4T1 group on the 22nd day, 29th day and 36th day (17.51±0.65g *vs* 18.45±2.14g, 17.65±1.02g *vs* 20.20±0.47g, 17.67±0.94g *vs* 20.02±0.42g, p<0.05). Compared with the wt 4T1 group, the body weight of mice in the CTX group was significantly reduced in the middle and late stage of drug administration (p<0.05, Fig. 1A left). There was no significant difference between the other groups and the wt 4T1 group (p>0.05, Fig. 1A left).

With the prolongation of administration time, the tumor volume of the Tα1 group increased compared with that of the wt 4T1 group, but the results showed no statistical difference. The tumor volume of the D-Gal group was slightly smaller than that of the wt 4T1 group (p>0.05, Fig. 1A right). The tumor volume in the DOX group was slightly smaller than that in the wt 4T1 group, and the tumor volume measured at the last dose week was significantly larger than that in the wt 4T1 group. The tumor volume of CTX group was significantly lower than that of wt 4T1 group (p<0.05, Fig. 1A right).The tumor volume of the nu 4T1 group was slightly smaller in the early stage than BALB nu group, but significantly increased in the later stage (on the 8th day, the 29th day and the 36th day, respectively. p<0.05, Fig. 1A right).

After 3 weeks of administration, the tumor metastasis was monitored by whole body Xenogen imaging, which demonstrated that all groups expect BALB wt and CTX groups exhibited a marked Xenogen imaging signal in the lungs (Fig. 1B). The luminescence intensity of the CTX positive drug control group was significantly lower than that of the wt 4T1 group, and there was a significant difference (p<0.05). Compared with the wt 4T1 group, the D-Gal group, the Tα1 group and the DOX group had macroscopic metastases in the lung tissues after 3 weeks of administration, especially in the Tα1 group. At the same time, the lung metastasis rate of the nu 4T1 group was as high as 100%, and the number of metastases was significantly higher than that of BALB nu mice. At 5 weeks of administration, lung metastases increased, especially in the DOX group. Thus thymus function status is closely related to the development and metastasis of breast cancer (Fig. 1C).

The thymus output function of breast cancer model mice was decreased

Mice were sacrificed at the third week and the fifth week of administration respectively. Blood was extracted from the fundus venous plexus, RNA was extracted, and the expression of TRECs in peripheral blood was detected by qPCR. The results show that the thymus output function of breast cancer model mice was decreased. In week 3 of administration, compared with wt 4T1 group, TRECs expression in all other groups had decreased, especially in D-Gal, Tα1 and CTX group (Fig. 2A). At 5 weeks

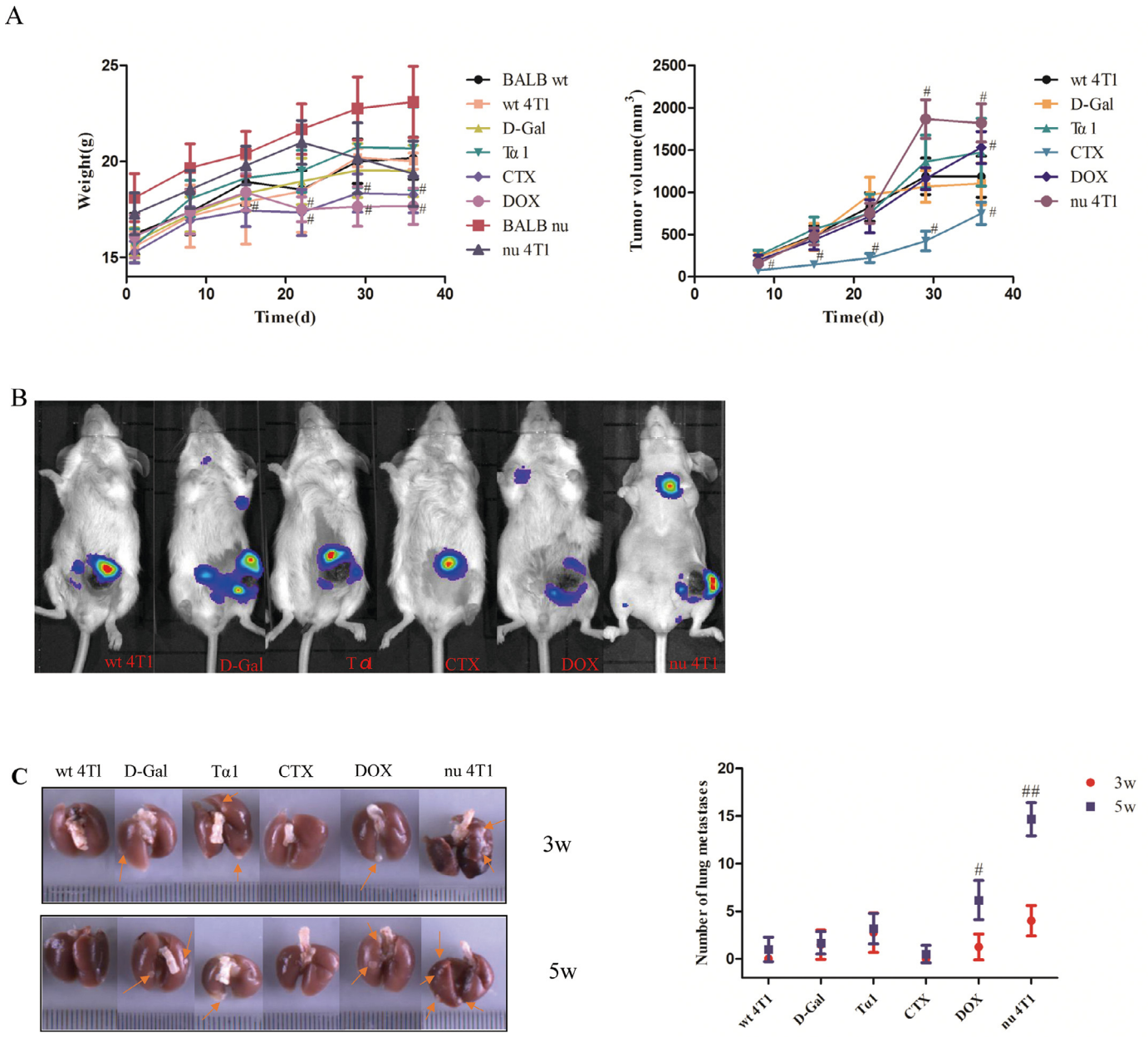

Fig. 1. Thymus function status is closely related to the development and metastasis of breast cancer. (A) The trend of weight change (left) and the tumor growth curve of 4T1 breast cancer bearing mice(right). Data are mean ± SD. $^{\#}p<0.05$, *vs* wt 4T1 group. (B) Representative living fluorescent imaging of tumor bearing mice after 3 weeks of administration. (C) Tumor metastasis in the lungs of mice administrate at the third week and the fifth week respectively (up: the third week; down: the fifth week). Data are means ± SEM. $^{\#}p<0.05$, $^{\#\#}p<0.01$, *vs* wt 4T1 group.

of administration, the expression of TRECs in each group decreased compared with 3 weeks of administration, especially in the wt 4T1 group and DOX group (Fig. 2A).

After 3 weeks of administration, compared with the BALB wt group, the lung, spleen, and thymus coefficients of the wt 4T1 group were increased to varying degrees. Compared with the wt 4T1 group, except for the Tα1 group, the lung and spleen coefficients of the other groups were slightly decreased. The lung coefficient and spleen coefficient of the CTX group and the spleen coefficient of the DOX group were significantly different from the wt 4T1 group. (Fig. 2B). Similarly, after 5 weeks of administration, compared with the BALB wt group, lung, spleen, and thymus coefficients of the wt 4T1 group were increased to varying degrees. Compared with the wt 4T1 group, the spleen coefficients of the CTX group and DOX group were significantly reduced, and the difference was statistically significant. Due to a large number of tumor metastases, the thymus coefficient of the DOX group was significantly higher than that of the wt 4T1 group. (Fig. 2C).

Histopathological changes of Lung, Tumor and Thymus tissues in tumor-bearing Mice

To explore the histopathological changes of tumor-bearing mice in each group, H&E staining was performed on the paraffin section of lung, tumor and thymus tissues. Pulmonary metastasis is the most common target organ of breast cancer. It can be seen from Fig. 3A that the alveolar structure is clear in the BALB wt group. The alveolar wall is thickened in the tissue section of the wt 4T1 group, the inflammatory cells infiltrated, and multiple metastatic tumor lesion areas appeared. D-Gal group alveolar wall structure was fuzzy, partially collapsed, metastasis area is large and more, a large number of inflammatory cells infiltration. Tα1 group micro-metastasis increased, there is a large area of metas-

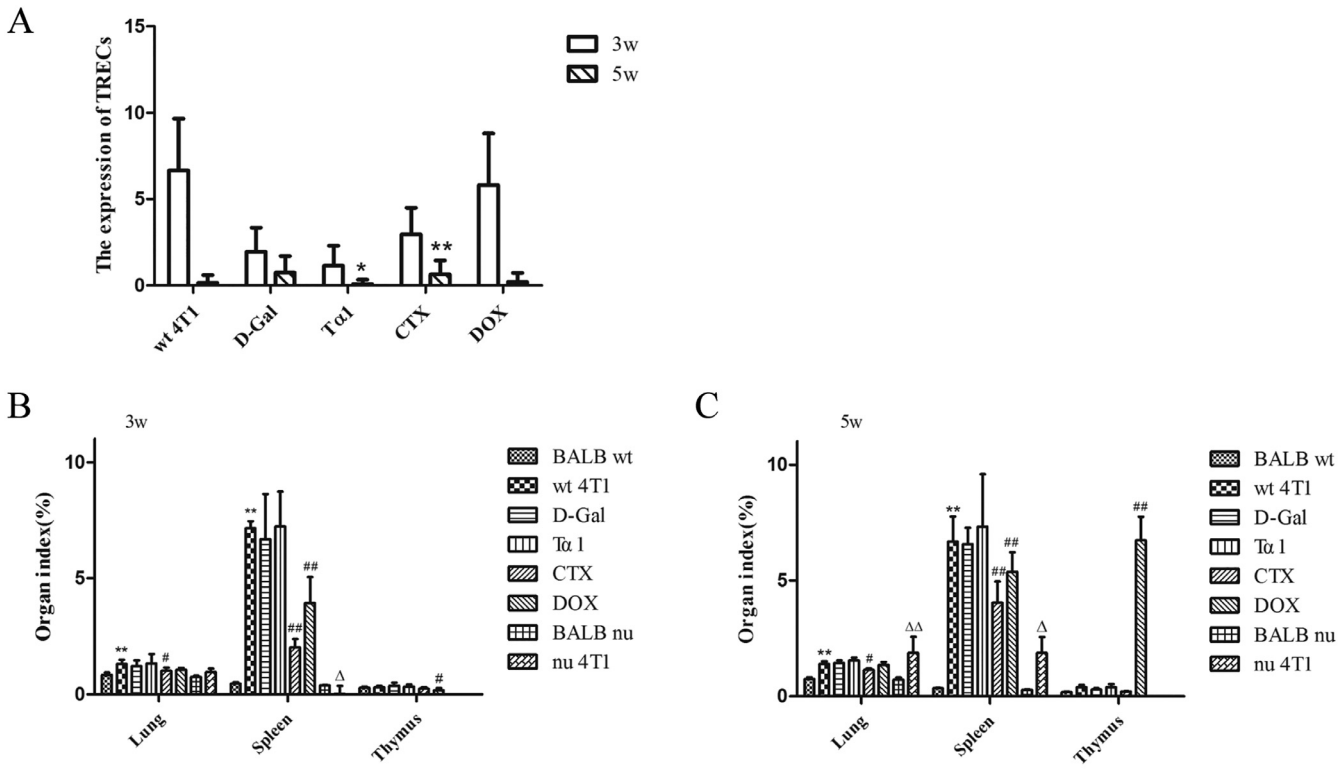

Fig. 2. The thymus output function of breast cancer model mice was decreased. (A) Changes of the expression of TRECs of each group after 3 weeks and 5 weeks administration. $^{*}p<0.05$, $^{**}p<0.01$, 3w *vs* 5w. Data are means ± SEM. (B) Organ indexes of each group after administration three weeks. Data are means ± SD, n=4. $^{*}p<0.05$, $^{**}p<0.01$, *vs* BALB wt group, $^{\#}p<0.05$, $^{\#\#}p<0.01$, *vs* wt 4T1 group, $^{\triangle}p<0.05$, $^{\triangle\triangle}p<0.01$, *vs* nu 4T1 group. (C) Organ indexes of each group after administration five weeks. Data are means ± SD, n=6. $^{*}p<0.05$, $^{**}p<0.01$, *vs* BALB wt group, $^{\#}p<0.05$, $^{\#\#}p<0.01$, *vs* wt 4T1 group, $^{\triangle}p<0.05$, $^{\triangle\triangle}p<0.01$, *vs* nu 4T1 group.

tases near the tracheal branches, and the surrounding normal alveolar structure was destroyed. CTX group alveolar structure is clear, close to normal tissue, metastases are small and the area of metastases is small, inflammatory cell infiltration is less. DOX group has clear alveolar structure, some inflammatory cells infiltrate, more micrometastases were observed in the later stage. HE staining of lung tissue showed that except for the CTX group and DOX group, the other groups lost normal tissue structure, and there was a large area of metastasis in the lung tissue of Tα1 group and nu 4T1 group. (Fig. 3A)

The tumor cells in the wt 4T1 group had different size and morphology, and their arrangement was disordered. The nucleus was deformed, showing lobular, nodular, and irregular shapes. The chromatin was significantly increased and thickened. The cells in D-Gal group had different morphology, tight arrangement, obvious nuclear deformity, and partial shrinkage and necrosis; tumor cells in Tα1 group had different nucleus sizes and obvious nuclear division; tumor cells in CTX group were loosely arranged and had deep spindle-like staining; In the DOX group, the nucleus was enlarged and the nuclear membrane was thickened. In the nu 4T1 group, the nucleus of tumor cells was obviously condensed and necrotic and lost its polarity. (Fig. 3B).

As an important immune organ of the body, the thymus is divided into multiple leaflets by the connective tissue capsule. Each leaflet is composed of thymocytes dense, darker cortical parts and medullary parts with more epithelial cells and lighter coloration. In the BALB wt group, the thymus showed clear structure and obvious cortical and medulla. The wt 4T1 group, D-Gal group and Tα1 group showed thinning and atrophy of the thymus tissue, and there was no obvious boundary between the cortex and medulla. The thymus atrophy in the DOX group was obvious, and the initial cortex medulla was disappeared. The D-Gal group and the DOX group were lightly colored, indicating that the number of lymphocytes in the tissue was small and the tissue was atrophied. High-power microscope observation showed that a large number of vesicular-like structures appeared in the tissues of D-Gal group, and neutrophils were scattered. The thymus tissue of the CTX group has a clear structure, and there is an eosinophilic thymus gland in the medulla. The thymus gland in the medulla of DOX group still exists, but it is very large and clearly visible, but the cell components are almost completely degraded, dyed into pink, and a large number of tumor cells appear in the medulla, and the nucleus has different forms and mitotic figures. (Fig. 3C).

PTMα and Tβ15b1 were the two genes with the most significant change

In this experiment, gene chip technology was used to comprehensively study the gene expression in different tumor tissue samples of mice (wt 4T1, D-Gal and BALB nu). A total of 25,655 gene expression changes were screened, and 94 genes were associated with thymus. In the D-Gal group up-regulated genes, the expression of PTMα was up-regulated by 33.86-fold, which was significantly higher than wt 4T1 group ($p<0.01$). The expression level of Tβ15b1 was significantly decreased, and the wt 4T1 group was about 10 times higher than D-Gal group ($p<0.01$). Similarly, in the BALB nu group compared with the wt 4T1 group, PTMα and Tβ15b1 were the two genes with the most significant up-regulation and down-regulation, respectively ($p<0.01$). Further analysis of the differentially expressed genes in 9 samples showed that the wt 4T1 group, D-Gal group, and BALB nu group were grouped into three categories, which further confirmed that changes in thymus function affected gene expression in breast cancer tissues of mice (Fig. 4A).

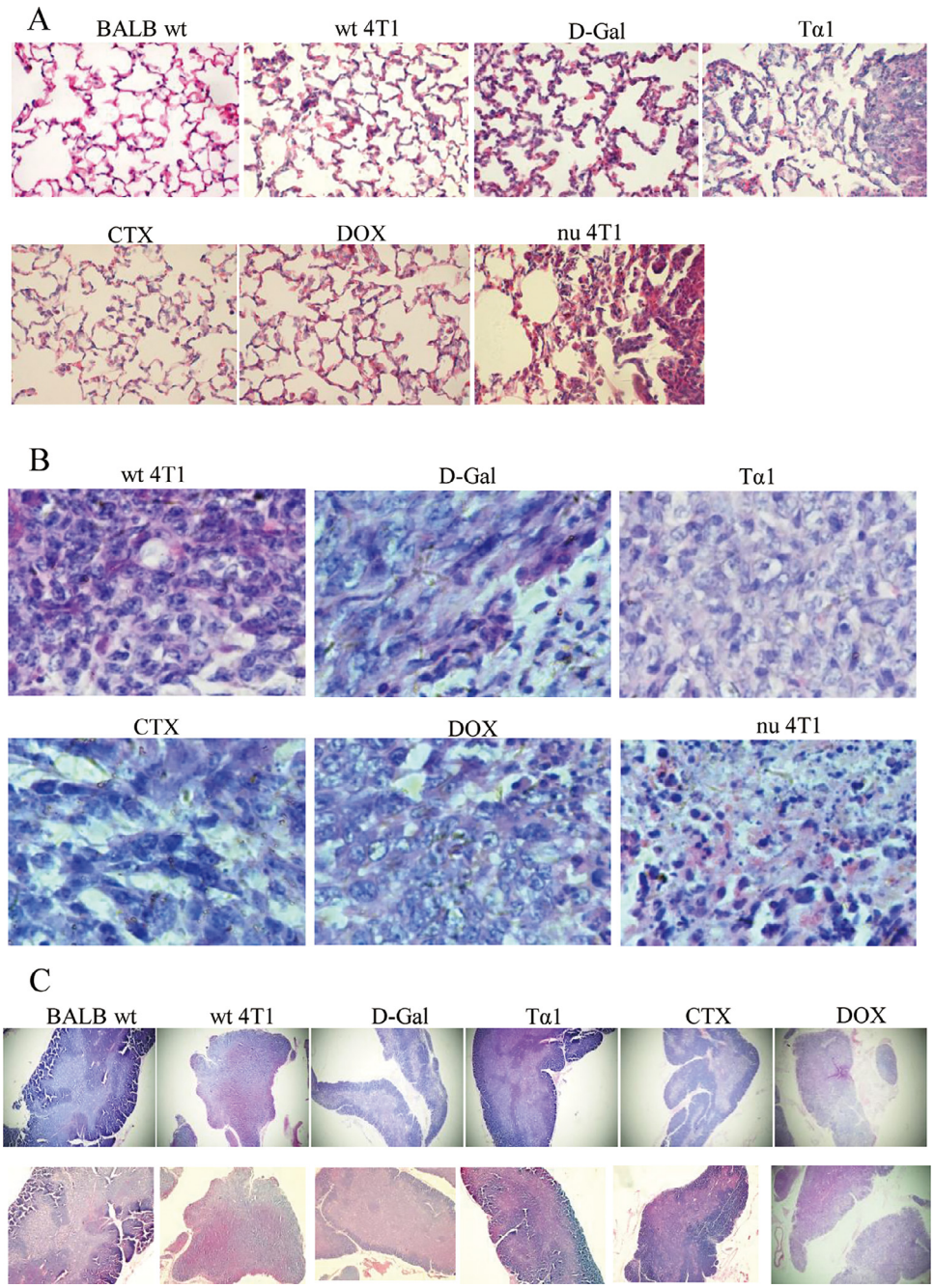

Fig. 3. Histopathological changes of Lung, Tumor and Thymus tissues in tumor-bearing Mice. (A) HE staining of lung tissue after 5 weeks administration (5w,400X).(B) HE staining of tumor tissue (5w,400X). (C) HE staining of thymus tissue (5w,40X.Up is 3w, down is 5w).

Peripheral blood thymus hormone expression level

The expression level of PTMα in peripheral blood showed a downward trend with the prolongation of administration time. After 5 weeks of administration, except for the CTX group, the expression levels of PTMα in the other groups were higher than those in the BALB wt group, especially in the Tα1 group. The expression level of Tβ15 in peripheral blood did not change significantly. Except Tα1 group, Tβ15 expression level also showed a downward trend. Pearson correlation coefficient analysis showed that the number of tumor lung metastasis was positively correlated with the expression level of Tβ15 (R=0.406, P=0.029) in serum at 3 weeks of administration. (Fig. 4B).

PTMα and Tβ15b1 gene expression changes effect of proliferation, invasion and migration of 4T1 breast cancer cells in vitro

Q-PCR showed the PTMα and Tβ15b1 gene overexpression and knocking down efficacy in 4T1 breast cancer cells . Q-PCR validates PTMα and Tβ15b1 gene overexpression / silence efficiency. (Fig. 5A). 4T1 itself expresses PTMα and Tβ15b1 at high levels, especially PTMα. After overexpression, although PTMα expression increased, there was no significant difference.

Effect of PTMα and Tβ15b1 gene overexpression / silencing on proliferation, invasion and migration of 4T1 breast cancer cells in vitro . To gain insight into the function of PTMα and Tβ15b1 in breast cancer progression, we applied MTT assays to test cell viability after overexpression / silencing PTMα and Tβ15b1 expression in 4T1 breast cancer cells lines, and results revealed no effect on cell growth. (Fig. 5B).

To investigate the effects of PTMα and Tβ15b1 expression on invasion and migration of breast cancer cells, transwell assay and wound healing were applied. The results of transwell assay showed that after Ad-PTMα virus infection, the number of cells passing through matrigel gel was slightly lower than Ad-GFP, and the cell invasion ability was

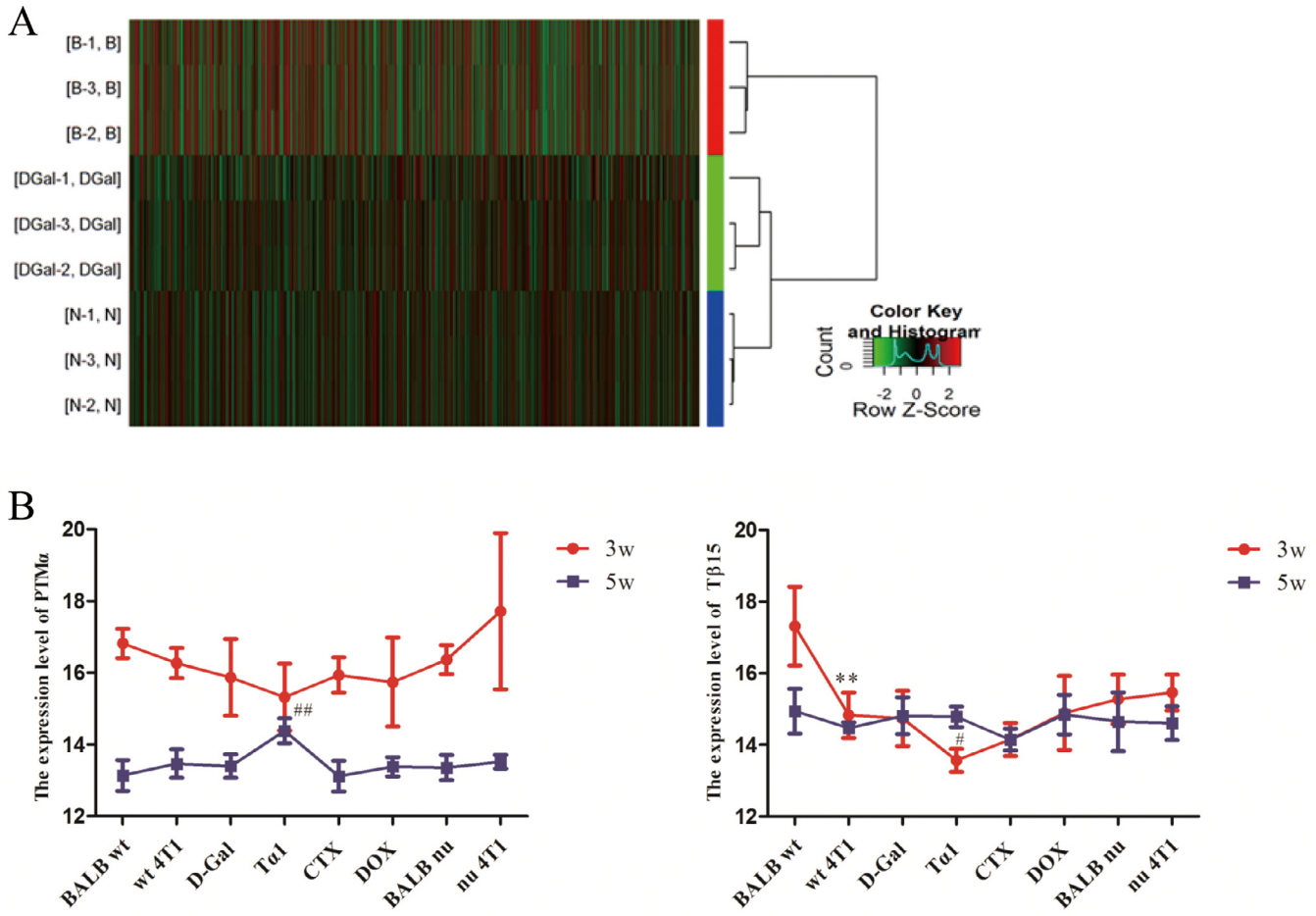

Fig. 4. PTMα and Tβ15b1 were the two genes with the most significant change. (A) Cluster analysis of differentially expressed genes. (B) Expression of PTMα and Tβ15 in peripheral blood at 3w and 5w. With the extension of administration time, the expression level of PTMα in peripheral blood showed a downward trend, and except Tα1 group, Tβ15 expression level also showed a downward trend. Data are means ± SD, n=3. *p<0.05, **p<0.01, *vs* BALB wt group, $^{\#}$p<0.05, $^{\#\#}$p<0.01, *vs* wt 4T1 group.

weakened. After Ad-Tβ15b1 virus infection, the number of cells passing through the gel was slightly increased, and the cell invasion ability was enhanced. PTMα-shRNA, Tβ15b1-shRNA virus infection, the number of cells that passed through increased compared with Si-GFP group, indicating that silencing PTMα and Tβ15b1 expression can enhance the invasion ability of 4T1-Luc cells (p>0.05, Fig. 5C-D). However, overexpression / silencing PTMα expression promoted cell migration. Overexpression Tβ15b1 decreased cell migration ability. Inversely, the ability was increased after Tβ15b1 silencing in 4T1 breast cancer cells (Fig. 5E-G).

Effects of PTMα and Tβ15b1 gene expression on tumor growth and metastasis in breast cancer-bearing mice. Another 80 BALB/c nude mice were randomly divided into 8 groups: BALB wt, wt 4T1, Ad-GFP, Ad-PTMα, Ad-Tβ15b1, Si-GFP, PTMα-shRNA and Tβ15b1-shRNA (n=10/group). 4T1-Luc cells infected with adenovirus or lentivirus were harvested respectively, resuspended in PBS, and analyzed by 0.4% trypan blue exclusion assay (viable cells, >95%). For breast cancer cell injection, approximately 1×10^{6} 4T1-Luc cells in 100μl PBS were injected into nude mice MFP. Each group of adenovirus-infected mice was injected with 10μl of the corresponding adenovirus solution at the tumor inoculation weekly to ensure the stability of gene expression. The measurement of the size of the primary tumor site, the calculation of tumor volume, organ coefficient and other methods are the same as above.

Weight, metastatic sites and organ index. The body weight of the mice was measured every 5 days after modeling. Compared with the Ad-GFP group, the weight of the Ad-PTMα group and the Ad-Tβ15b1 group decreased, and the weight of the Ad-Tβ15b1 mice was statistically significant on the 11th, 26th, and 31st, respectively, after inoculating (p<0.05). Compared with the Si-GFP group, the weight of the PTMα-shRNA group increased slightly (p>0.05), and the body weight of the Tβ15b1-shRNA group did not change significantly. (Fig. 6A). Compared with the Ad-GFP group, the tumor of Ad-PTMα and Ad-Tβ15b1 mice grew faster in the early stage. Especially in the Ad-Tβ15b1 group, which promoted the tumor growth slightly in the early stage but inhibited its growth at the later stage. Compared with the Si-GFP group, both PTMα-shRNA and Tβ15b1-shRNA inhibited tumor growth, but have not a statistically significant. (Fig. 6B).

In vivo fluorescence imaging data of small animals showed early metastasis in the Ad-PTMα group, the Ad-Tβ15b1 group, the Si-GFP group and the PTMα-shRNA group. Compared with Ad-GFP group, the luminescence intensity of the in situ tumor was lower in the Ad-PTMα group and the Ad-Tβ15b1 group, especially in the Ad-PTMα group. Compared with the Si-GFP group, the PTMα-shRNA and Tβ15b1-shRNA group had lower luminescence intensity. (Fig. 6C). Five weeks after tumor inoculation, the mice were sacrificed and the lung tissues were dissected. The 10% formalin solution was fixed and the metastases on the surface of the lung tissues were observed. The lung metastasis observed in all the wt 4T1 groups. The lung metastasis rate of the Ad-PTMα group,

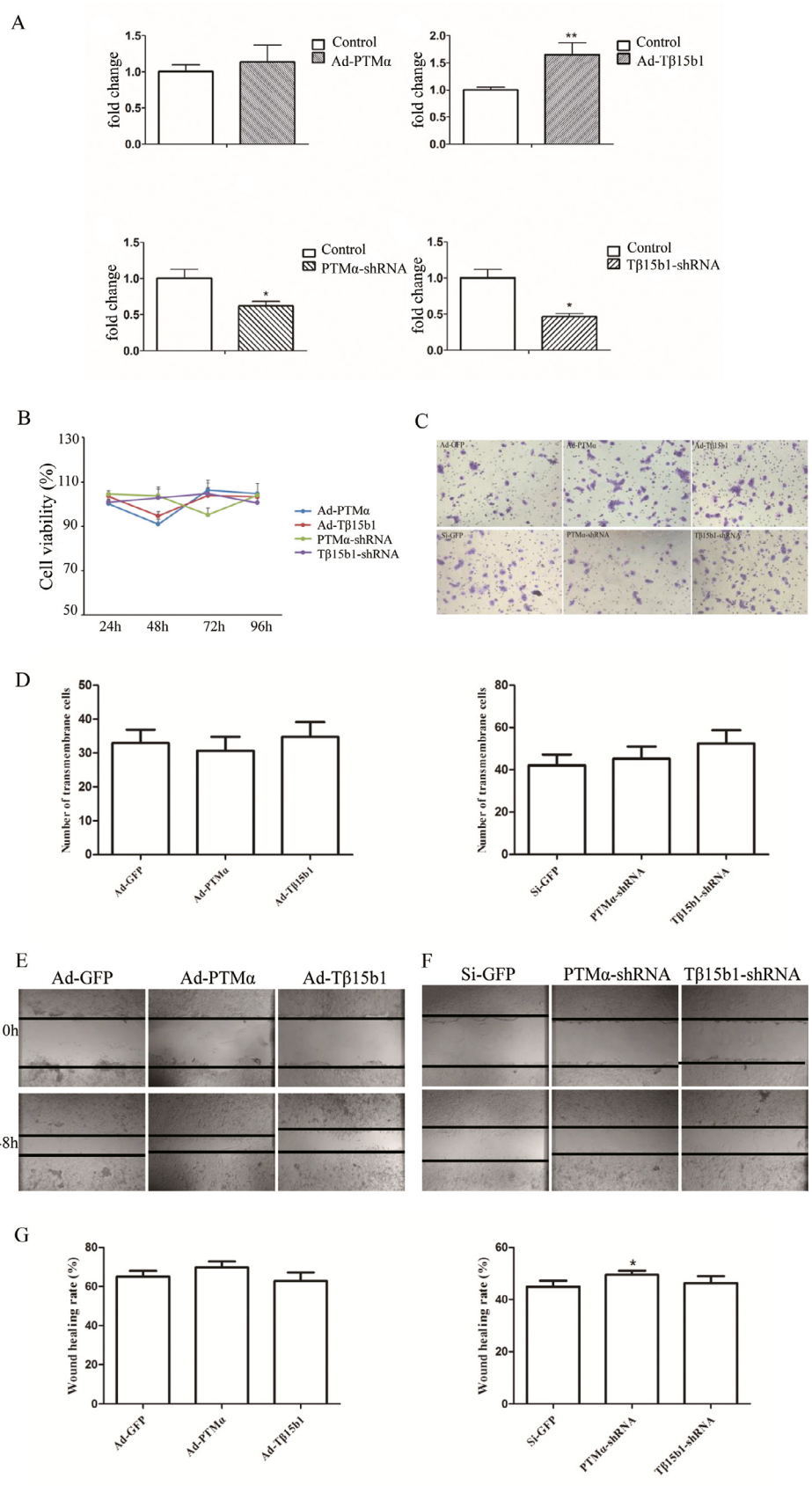

Fig. 5. Effect of PTM*α* and T*β*15b1 gene expression changes on proliferation, invasion and migration of 4T1 breast cancer cells in vitro. (A) qPCR validates PTM*α* and T*β*15b1 gene overexpression / silence efficiency. (B) MTT assay of the viability of 4T1 breast cancer cells lines treated with overexpression / silencing PTM*α* and T*β*15b1 for different time. (C) Transwell assay of 4T1 breast cancer cells lines treated with overexpression / silencing PTM*α* and T*β*15b1 for 48h. Ad-GFP and Si-GFP as control respectively. (D)Transmembrane cells were counted in five random fields. (I) Wound healing of 4T1 breast cancer cells lines treated with overexpression / silencing PTM*α* and T*β*15b1 for 48h. Ad-GFP and Si-GFP as control respectively. (G)Statistical chart of wound healing rate. Three independent experiments were performed, and the results are presented with the means ± SEM, $^{*}p<0.05$, $^{**}p< 0.01$, *vs* control group.

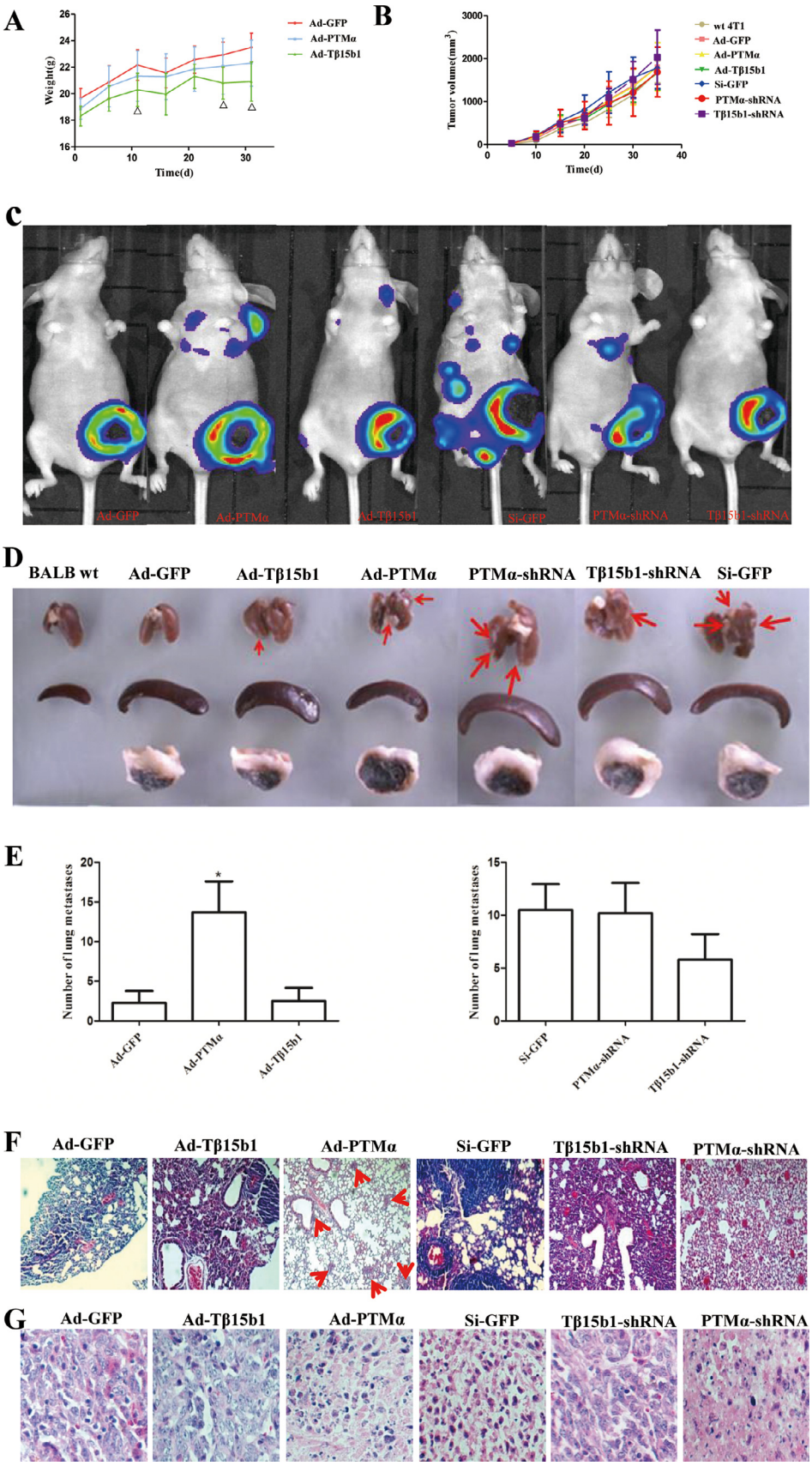

Fig. 6. PTM*α* and T*β*15b1 overexpression promotes tumor metastasis, silencing inhibit tumor metastasis. (A)The trend of weight change of 4T1 breast cancer bearing mice. Data are means ± SD, n=6. △P<0.05, *vs* Ad-GFP group. (B) The trend of the tumor growth curve of 4T1 breast cancer bearing mice. Data are means ± SD, n=6. (C)Representative living fluorescent imaging of tumor bearing mice after 3 weeks of administration. (D) Effects of PTM*α* and T*β*15b1 gene expression changes on organs of BALB/c nude mice (lung, spleen, tumor tissue). (E) Number of lung metastases after PTM*α* and T*β*15b1 gene expression changes. Data are means ± SEM. *P<0.05, *vs* Ad-GFP group. (F)H&E staining of lung tissue after 5 weeks administration. (G)H&E staining of tumor tissue(5w,400X).

Si-GFP group, PTMα-shRNA group and Tβ15b1-shRNA group was as high as 100%. Counting the number of lung metastases, the number of metastases in the Ad-PTMα group and the Ad-Tβ15b1 group was significantly higher than that in the Ad-GFP, especially in the Ad-PTMα group ($p<0.05$). (Fig. 6D-E). Metastasis was lower in the PTMα-shRNA group and the Tβ15b1-shRNA group than in Si-GFP group, and the difference was not statistically significant.

Effects of morphology on lung and tumor tissues of tumor-bearing mice. To explore the tumor metastasis of breast cancer in each group, H&E staining was performed on the paraffin section of lung and tumor tissues. Compared with the Ad-GFP group, the lung tissues of mice in the Ad-PTMα group showed smaller and more metastases, and the alveolar structure was clear. In the Ad-Tβ15b1 group, there were more metastases, thickened alveolar walls and less normal alveolar structures. Compared with the Si-GFP group, the PTMα-shRNA group showed fewer lung metastases and clear alveolar structure. The lung tissue metastasis was slightly smaller in the Tβ15b1-shRNA group, and the alveolar wall structure was not clear. (Fig. 6F). As shown in Fig. 6G, the tumor cells in Ad-GFP group, Ad-Tβ15b1 group, and Tβ15b1-shRNA group were well aligned with obvious mitosis. In the Ad-PTMα group, the nucleus pyknosis, cytoplasm increased, and cell polarity was lost, especially in the PTMα-shRNA group.

Discussion

Our study showed that thymus function status is closely related to the development and metastasis of breast cancer. We use BALB wt, BALB nu, wt 4T1, nu 4T1, D-Gal, Tα1, CTX, Dox in this research. As a central immune organ, the function and state of the thymus directly affect the differentiation and function of T lymphocytes of the immune system. Aging degeneration of the thymus is the direct cause of immune aging [14]. D-Gal aging model is a commonly used model for pharmacological study of anti-aging drugs. The experiment results show that, compared with wt 4T1 group, D-Gal group decreased TRECs expression in peripheral blood in mice, the drug delivery late mice thymus atrophy, thymus index, spleen index is slightly reduced, increased pulmonary metastasis rate, slightly increased lung metastases, lung tissue HE staining showed thickening of alveolar walls, alveolar atrophy, loss of normal structure, tumor metastases and the area is large, consistent with literature reports [15]. It is suggested that the aging of thymus gland induced by D-Gal promotes lung metastasis of tumor in mice.

DOX is a commonly used clinical anti-tumor antibiotic with a broad anti-tumor spectrum. Our results showed that the spleen index and thymus index of DOX group were significantly reduced and the number of tumor lung metastases was increased at 3 weeks after DOX administration than wt 4T1 group. At 5 weeks of administration, the spleen index was slightly lower, the thymus index was significantly higher, and the number of lung metastases was significantly increased. Combined with HE staining of thymus tissue, it was found that cortical parts of the DOX group were significantly thinner and atrophic, with disordered cell arrangement, and a large number of tumor cells appeared in the medulla at the later stage, with distinct nuclear morphology and obvious mitosis. Therefore, early DOX group reduced thymus coefficient to a level far lower than that of the BALB wt group, which may be detrimental to the normal immune function of the body. Pathological enlargement of immune organs caused by tumor in later stage may further promote the development of tumor.

Tα1, as a biological reaction modifier, has been in preclinical and clinical trials, and is used alone or in combination with cytokines and chemotherapy for malignant tumors, such as stage IV malignant melanoma, hepatocellular carcinoma, and breast cancer, etc. [16–18]. Yuan et al. [19] showed that Tα1 treatment alone could not inhibit tumor growth in tumor-bearing mice. Tα1 not only promoted the increase of $CD8^+$ T cells, but also enhanced the immunosuppressive function of MDSC, leading to the inhibition of T cell responses and ultimately impaired anti-tumor efficacy. In this study, it was also found that the tumor weight and volume of the Tα1 group was heavier and larger than wt 4T1 group. Lung metastasis is early and frequent. Although Tα1 can improve the immunosuppressive state of the tumor, it is not helpful to inhibit the metastasis of mouse breast cancer when used alone in the early stage of tumor development.

TRECs as a Marker of Thymic Function [20], which is a by-product of the rearrangement of TCR genes and is free DNA. TRECs is stably present in cells, not amplified with the proliferation of T cells, but continuously diluted with the division of T cells. By quantitatively detecting the copy number of TRECs in DNA, the content of TRECs in T cells can be calculated and its recent thymic output function can be understood [21]. In this experiment, the expression level of TRECs in peripheral blood of mice in each group was detected by qPCR. It was found that at the initial stage of drug administration, the immune response of the body was active, and the expression level of TRECs in peripheral blood of each group decreased with the growth of tumor.

In order to further study the changes of gene expression in breast cancer mice with different thymus function, a total of 25655 genes were screened from mouse tumor tissue samples by gene microarray technology. Among them, there were PTMα, Tβ15b1, Tβ4x, Tβ10, Ptms, Tmpo, etc., especially PTMα and Tβ15b1. The expression level of PTMα in the D-Gal group was 33.86 times higher than that in wt 4T1 group, and the expression level of Tβ15b1 was down to about 1/10 of that in the wt 4T1 group. Similarly, the PTMα and Tβ15b1 gene expressions in BALB nu and wt 4T1 group were significantly up-regulated and down-regulated, respectively. In order to further explore the role of these genes in the development of breast cancer and the specific mechanisms, we finally screened the PTMα and Tβ15b1 genes based on the bioinformatics analysis and literature reports of breast cancer-related genes. Studies have shown that thymosin β15A (Tβ15A) is a predictor of chemotherapy response in triple-negative breast cancer [22]. Tβ15 is also detected in human prostate and prostate cancer tissues, as well as in normal colon and colon cancer tissues [23]. We detected the expression levels of these two thymosins in peripheral blood by ELISA: the smaller the change of PTMα expression in peripheral blood, the more obvious the tumor metastasis. Pearson correlation coefficient analysis showed that the number of tumor metastasis was positively correlated with the expression level of Tβ15 ($R=0.406$, $P=0.029$) in serum at 3 weeks of drug administration.

In this study, transwell chamber and wound healing assays showed that increased PTMα expression could weaken the invasion ability of cells and enhance the migration ability. Overexpression of Tβ15b1 enhanced the ability of cell invasion and decreased the ability of cell migration. Silencing of PTMα and Tβ15b1 genes enhanced cell invasion and migration. Combined with the results of ELISA and the count of tumor lung metastases, it can be speculated that the silencing of PTMα gene and Tβ15b1 gene leads to the decrease of corresponding thymosin expression in peripheral blood, which will promote the metastasis of breast cancer.

BALB/c mice transplantation of 4T1 breast cancer metastasis model was constructed by using fluorescence reporter group labeled cells and combined with fluorescence imaging technology in vivo to observe the growth and metastasis of tumor cells in vivo in real time. In this study, nude mice from the same source of BALB/c were used as the model, and the interference of thymus hormone secreted by the thymus tissue itself was excluded, and 4T1-Luc breast cancer cells with overexpression/silencing of PTMα and Tβ15b1 genes were respectively inoculated under the pad of breast fat in the second-last pair of mice. Previous studies have shown that high PTMα mRNA expression is detected in colon cancer, liver cancer, neuroblastoma, rhabdomyosarcoma, and well-differentiated thyroid cancer at the mRNA level [24–27], on the other hand, at the protein level, the results of cancer tissues confirm the fact that aggressive tumors contain more PTMα, which can be detected in breast tumors, colon cancer, and urinary tumors, and has the potential role as a novel proliferation marker for tumor development. In ad-

dition, Tβ15b1 can also be used as a predictive indicator of chemotherapy response in triple-negative breast cancer, and its expression can be detected in both colon cancer and prostate cancer. Our experimental study found that overexpression of PTMα gene promoted tumor in situ growth and distant metastasis. Overexpression of Tβ15b1 can promote distant metastasis and inhibit in situ tumor growth in late stage. Silencing of PTMα, Tβ15b1 gene inhibited distant metastasis and promoted in situ growth, especially after silencing of Tβ15b1 gene. In vitro results showed that the invasion and metastasis of 4T1 cells were decreased after the silencing of PTMα and Tβ15b1 genes, which was inconsistent with the results in vivo.

4T1 cells themselves express higher PTMα and Tβ15b1, so the effect is not obvious in the case of overexpression. The PTMα gene overexpression in the mouse model only promotes tumor growth and lung metastasis in the early stage, and has no significant effect on tumor growth and metastasis in the later stage; Tβ15b1 overexpression promotes tumor growth in the early stage and inhibits its growth in the later stage; Tβ15b1 gene silencing inhibits tumor lung metastasis. At the cellular level, Tβ15b1 silencing increases migration capacity.

In short, thymic function affects breast cancer development and metastasis, it may be through regulating expression of PTMα and Tβ15b1 in thymus, and subsequently influencing the invasion and metastasis of tumor cells. Our study provided new directions for breast cancer therapy.

Funding

This work was supported by the Zhejiang Provincial Natural Science Foundation of China under Grant No. LY19H280010 to K He, Zhejiang Provincial Key Laboratory Project (grant no. 2012E10002), Opening Project of Zhejiang Provincial Preponderant and Characteristic Subject of Key University (Traditional Chinese Pharmacology) to Zhejiang Chinese Medical University (No. ZYAOX2018015), Young and Middle-aged Scientific Research and Innovation Fund Project of Zhejiang Chinese Medical University (No.KC201916) and National Natural Science Foundation of China (81473575 to JL Gao).

Declaration of Competing Interest

The authors declare that they have no known competing financial interests or personal relationships that could have appeared to influence the work reported in this paper.

CRediT authorship contribution statement

Dongling Shi: Formal analysis, Writing - original draft, Writing - review & editing, Funding acquisition. **Yanmei Shui:** Methodology, Validation, Formal analysis. **Xie Xu:** Validation, Investigation. **Kai He:** Investigation, Funding acquisition. **Fengqing Yang:** Conceptualization, Supervision. **Jianli Gao:** Conceptualization, Writing - review & editing, Supervision, Funding acquisition.

References

[1] A. Rocca, A. Schirone, R. Maltoni, S. Bravaccini, L. Cecconetto, A. Farolfi, G. Bronte, D. Andreis, Progress with palbociclib in breast cancer: latest evidence and clinical considerations, Therapeut. Adv. Med. Oncol. 9 (2) (2017) 83–105.
[2] D.C. Douek, R.A. Koup, Evidence for thymic function in the elderly, Vaccine 18 (16) (2000) 1638–1641.
[3] R.H. Johnson, C.K. Anders, J.K. Litton, K.J. Ruddy, A. Bleyer, Breast cancer in adolescents and young adults, Pediatr. Blood Cancer 65 (12) (2018) e27397.
[4] I. Erić, A. Petek Erić, J. Kristek, I. Koprivčić, M. Babić, Breast cancer in young women:pathologic and immunohistochemical features, Acta Clin. Croatica 57 (3) (2018) 497–502.
[5] R. Danielli, F. Cisternino, D. Giannarelli, L. Calabrò, R. Camerini, V. Savelli, G. Bova, R. Dragonetti, A.M. Di Giacomo, M. Altomonte, M. Maio, Long-term follow up of metastatic melanoma patients treated with Thymosin alpha-1: investigating immune checkpoints synergy, Expert Opin. Biol. Ther. 18 (sup1) (2018) 77–83.
[6] P.Y. Wang, The Biosynthesis of Thymosin α1 and the Analysis of its Anti-Tumor Mechanicsim[D], Zhejiang University, 2012.
[7] H.J. Cha, M.J. Jeong, H.K. Kleinman, Role of thymosin beta4 in tumor metastasis and angiogenesis, J. Natl. Cancer Inst. 95 (22) (2003) 1674–1680.
[8] W.S. Wang, P.M. Chen, H.L. Hsiao, H.S. Wang, W.Y. Liang, Y. Su, Overexpression of the thymosin beta-4 gene is associated with increased invasion of SW480 colon carcinoma cells and the distant metastasis of human colorectal carcinoma, Oncogene 23 (39) (2004) 6666–6671.
[9] K.O. Hong, J.I. Lee, S.P. Hong, S.D. Hong, Thymosin β4 induces proliferation, invasion, and epithelial-to-mesenchymal transition of oral squamous cell carcinoma, Amino acids 48 (1) (2016) 117–127.
[10] S. Sribenja, K. Sawanyawisuth, R. Kraiklang, C. Wongkham, K. Vaeteewoottacharn, S. Obchoei, Q. Yao, S. Wongkham, C. Chen, Suppression of thymosin β10 increases cell migration and metastasis of cholangiocarcinoma, BMC Cancer 13 (2013) 430.
[11] W. Theunissen, D. Fanni, S. Nemolato, E. Di Felice, T. Cabras, C. Gerosa, P. Van Eyken, I. Messana, M. Castagnola, G. Faa, Thymosin beta 4 and thymosin beta 10 expression in hepatocellular carcinoma, Eur. J. Histochem. EJH 58 (1) (2014) 2242.
[12] Y.M. Gu, S.Y. Li, X.S. Qiu, E.H. Wang, Elevated thymosin beta15 expression is associated with progression and metastasis of non-small cell lung cancer, APMIS: Acta Pathologica, Microbiologica, Et Immunologica Scandinavica 116 (6) (2008) 484–490.
[13] C. Wang, Y.G. Chen, J.L. Gao, G.Y. Lyu, J. Su, Q.I. Zhang, X. Ji, J.Z. Yan, Q.L. Qiu, Y.L. Zhang, L.Z. Li, H.T. Xu, S.H. Chen, Low local blood perfusion, high white blood cell and high platelet count are associated with primary tumor growth and lung metastasis in a 4T1 mouse breast cancer metastasis model, Oncol. Lett. 10 (2) (2015) 754–760.
[14] K.F. Azman, R. Zakaria, D-Galactose-induced accelerated aging model: an overview, Biogerontology 20 (6) (2019) 763–782.
[15] S. Rivankar, An overview of doxorubicin formulations in cancer therapy, J. Cancer Res. Therapeut. 10 (4) (2014) 853–858.
[16] S.J. Fang, L.Y. Zheng, Z.W. Zhao, X.X. Fan, M. Xu, J.S. Ji, [Effect of transcatheter arterial chemoembolization combined with thymosin alpha 1 on the autophagy of immune cells from advanced hepatocellular carcinoma], Zhonghua yi xue za zhi 97 (25) (2017) 1942–1946.
[17] X. Lao, B. Li, M. Liu, C. Shen, T. Yu, X. Gao, H. Zheng, A modified thymosin alpha 1 inhibits the growth of breast cancer both in vitro and in vivo: suppressment of cell proliferation, inducible cell apoptosis and enhancement of targeted anticancer effects, Apoptosis: Int. J. Program. Cell Death 20 (10) (2015) 1307–1320.
[18 C. Yuan, Y. Zheng, B. Zhang, L. Shao, Y. Liu, T. Tian, X. Gu, X. Li, K. Fan, Thymosin α1 promotes the activation of myeloid-derived suppressor cells in a Lewis lung cancer model by upregulating Arginase 1, Biochem. Biophys. Res. Commun. 464 (1) (2015) 249–255.
[19] S. Darb-Esfahani, R. Kronenwett, G. von Minckwitz, C. Denkert, M. Gehrmann, A. Rody, J. Budczies, J.C. Brase, M.K. Mehta, H. Bojar, B. Ataseven, T. Karn, E. Weiss, D.M. Zahm, F. Khandan, M. Dietel, S. Loibl, Thymosin beta 15A (TMSB15A) is a predictor of chemotherapy response in triple-negative breast cancer, Br. J. Cancer 107 (11) (2012) 1892–1900.
[20] D.P. Wu, Y. Wang, H.R. Chang, Z.L. Zhu, Y.F. Feng, Study on the Establishement of Quantitative PCR and Run-off PCR for Evaluating Thymic Output and Immune reconstitution, J. Soochow Univ. (Med. Ed.) 29 (01) (2009) 112–115.
[21] A.P. Chidgey, R.L. Boyd, Stemming the tide of thymic aging, Nat. Immunol. 7 (10) (2006) 1013–1016.
[22] J. Banyard, C. Barrows, B.R. Zetter, Differential regulation of human thymosin beta 15 isoforms by transforming growth factor beta 1, Genes, Chromosomes Cancer 48 (6) (2009) 502–509.
[23] M. Mori, G.F. Barnard, R.J. Staniunas, J.M. Jessup, G.D. Steele Jr., L.B. Chen, Prothymosin-alpha mRNA expression correlates with that of c-myc in human colon cancer, Oncogene 8 (10) (1993) 2821–2826.
[24] C.G. Wu, N.A. Habib, R.R. Mitry, P.H. Reitsma, S.J. van Deventer, R.A. Chamuleau, Overexpression of hepatic prothymosin alpha, a novel marker for human hepatocellular carcinoma, Br. J. Cancer 76 (9) (1997) 1199–1204.
[25] H. Sasaki, Y. Sato, S. Kondo, I. Fukai, M. Kiriyama, Y. Yamakawa, Y. Fujii, Expression of the prothymosin alpha mRNA correlated with that of N-myc in neuroblastoma, Cancer Lett. 168 (2) (2001) 191–195.
[26] K.A. Carey, D. Segal, R. Klein, A. Sanigorski, K. Walder, G.R. Collier, D. Cameron–Smith, Identification of novel genes expressed during rhabdomyosarcoma differentiation using cDNA microarrays, Pathol. Int. 56 (5) (2006) 246–255.
[27] K.P. Letsas, G. Vartholomatos, C. Tsepi, A. Tsatsoulis, M. Frangou-Lazaridis, Fine-needle aspiration biopsy-RT-PCR expression analysis of prothymosin alpha and parathymosin in thyroid: novel proliferation markers, Neoplasma 54 (1) (2007) 57–62.